

# Evaluation of biomimetic hyaluronic-based hydrogels with enhanced endogenous cell recruitment and cartilage matrix formation

*Acta Biomaterialia*. 2020 Jan 1; 101:293-303

*Vainieri M.L.*

*Lolli A.*

*Kops N.*

*D'Atri D.*

*Eglin D.*

*Yayon A.*

*Alini M.*

*Grad S.*

*Sivasubramaniyan K.*

*van Osch G.J.V.M.*

## ABSTRACT

Biomaterials play a pivotal role in cell-free cartilage repair approaches, where cells must migrate through the scaffold, fill the defect, and then proliferate and differentiate facilitating tissue remodeling. Here we used multiple assays to test the influence of chemokines and growth factors on cell migration and cartilage repair in two different hyaluronan (HA)-based hydrogels. We first investigated bone marrow Mesenchymal Stromal Cells (BMSC) migration *in vitro*, in response to different concentrations of platelet-derived growth factor-BB (PDGF-BB), chemokine ligand 5 (CCL5/RANTES) and stromal cell-derived factor 1 (SDF-1), using a 3D spheroid-based assay. PDGF-BB was selected as most favourable chemotactic agent, and MSC migration was assessed in the context of physical impediment to cell recruitment by testing Fibrin-HA and HA-Tyramine hydrogels of different cross-linking densities. Supplementation of PDGF-BB stimulated progressive migration of MSC through the gels over time. We then investigated *in situ* cell migration into the hydrogels with and without PDGF-BB, using a cartilage-bone explant model implanted subcutaneously in athymic mice. *In vivo* studies show that when placed into an osteochondral defect, both hydrogels supported endogenous cell infiltration and provided an amenable microenvironment for cartilage production. These processes were best supported in Fibrin-HA hydrogel in the absence of PDGF-BB. This study used an advanced preclinical testing platform to select an appropriate microenvironment provided by implanted hydrogels, demonstrating that HA-based hydrogels can promote the initial and critical step of endogenous cell recruitment and circumvent some of the clinical challenges in cartilage tissue repair.

**Keywords:** Biomaterials, cell migration, osteochondral defect model, endogenous cell recruitment, cartilage repair

### Statement of significance

The challenge of articular cartilage repair arises from its complex structure and architecture, which confers the unique mechanical behavior of the extracellular matrix. The aim of our research is to identify biomaterials for implants that can support migration of endogenous stem and progenitor cell populations from cartilage and bone tissue, in order to permanently replace damaged cartilage with the original hyaline structure.

Here, we present an *in vitro* 3D spheroid-based migration assay and an osteochondral defect model, which provide the opportunity to assess biomaterials and biomolecules, and to get stronger experimental evidence of the not well-characterized dynamic process of endogenous cells colonization in an osteochondral defect. Furthermore, the delicate step of early cell migration into biomaterials towards functional tissue engineering is reproduced. These tests can be used for pre-clinical testing of newly developed material designs in the field of scaffold engineering.

## INTRODUCTION

Articular cartilage is a load bearing tissue with a unique composition and structure. Once damaged, its poor intrinsic repair ability results in permanent functional impairment, which often leads to osteoarthritis in absence of treatment [90, 91]. A number of studies have shown limited cell infiltration of the cartilage tissue as an impediment to endogenous repair [88]. Effective management of cartilage lesions can be challenging, creating a burden for both patients and clinicians. With conservative treatment being unsuccessful, surgical interventions are proposed for articular cartilage lesions, such as microfracture or osteochondral allograft transplantation. When perforations penetrating the subchondral bone are created in the context of marrow stimulating techniques (microfracture), invading cells often exhibit limited healing potential, producing a fibrocartilaginous tissue with poor mechanical properties, rather than hyaline cartilage [16]. To overcome this issue, cell delivery approaches like autologous chondrocyte implantation and matrix-induced autologous chondrocyte implantation (ACI, MACI), have been established as cartilage repair methods [5-7]. Recently clinical interventions based on autologous mesenchymal stromal cells (MSCs) transplantation have been proposed [92-94]. When evaluating studies comparing patients treated with ACI/MACI and with autologous bone marrow derived MSCs, similar improvements were reported in relation to clinical outcome and pain score [23, 24]. Nonetheless these cell-based therapies face important limitations, due to enormous costs for the patients as well as cell handling, time and regulation related to safety [31]

The extracellular matrix (ECM) of articular cartilage is a highly functional dense connective tissue, but its restrictive barriers impede endogenous cell migration. Partial degradation of the ECM at the wound edge of the cartilage has been proposed to reduce its stiffness [95-97] and enhance endogenous cell migration. Although these findings have shown that cells, that are normally trapped in the dense ECM, are capable of initiating tissue repair once they reach the edge of the lesion, in terms of diarthroidal joint studies have suggested that cells might normally come from bone and bone marrow side and even from synovium [98, 99]. The induction of cell mobility to recruit cells into the defect is an attractive option that has already been described for *in situ* regeneration of multiple tissues [66, 98], in order to circumvent issues related to cell-based therapy. There is a pressing need to identify the optimal biomaterials [100] and recruitment factors that can be used as a cell free approach for cartilage regeneration strategies. A variety of scaffolds and bioactive compounds were shown to promote stem and progenitor cell recruitment and improve cell differentiation [88, 101]. However, to date, no studies have identified the effective biomaterial that would promote the recruitment and differentiation of endogenous stem/progenitor cells to achieve functional cartilage regeneration *in situ*.

Hyaluronan (HA) is a component of the cartilage matrix that has both chondro-protective and chondro-inductive properties [55]. HA-based biomaterials have been shown to enhance healing processes in osteochondral defects in rabbit and minipig models [102, 103]. They possess a unique biochemical composition that recreates the embryonic-like microenvironment [56], which may be favorable for the regenerative process. HA-based hydrogels can be enzymatically cross-linked *in situ*, rendering the system safely injectable and non-invasive [60, 104]. HA-Tyramine (HA-Tyr) hydrogels have been developed as drug carriers for protein delivery [57, 105] and for tissue engineering applications [58]. It is known that by tuning the hydrogel the microenvironment can be modulated, which in turn can regulate spatial cell organization and matrix biosynthesis. HA-Tyr conjugates have advantageous material chemistry perspectives, the system is enzymatically cross-linked via a reaction catalyzed by horseradish peroxidase (HRP) using hydrogen peroxide ( $H_2O_2$ ) as substrate. The fine tuning of its mechanical strength can be achieved by the  $H_2O_2$  concentration without affecting the gelation rate [105]. It has been shown that varying the HA-Tyr hydrogel cross-linking density can modulate MSC differentiation and matrix biosynthesis [59]. Fibrin-HA (FB/HA) combination is widely used in tissue engineering and the specific conjugation of FB/HA hydrogel (Regenogel™), is well known for its applications in the regeneration of various tissues, such as cartilage and intervertebral disc [60, 66, 106]. The particular method employed for conjugation of HA to fibrinogen allows high versatility of the resulting hydrogels by alternating the molecular weight of HA, degree of activation and Fibrinogen/HA ratio. The resulting hydrogels are particularly stable compared to other Fibrin based scaffolds with remarkably lower rate of degradation of fibrin and a larger mesh size, thus allowing better cell migration and ECM deposition [60].

This study uses a sequence of assays to compare different HA-containing hydrogels for cell mobility, differentiation and matrix deposition. We evaluated the ability of human bone marrow stromal cells (hBMSCs) to migrate in a hydrogel under the influence of different chemokines, i.e. PDGF-BB, RANTES and SDF-1 in a 3D spheroid-based assay. After selecting PDGF-BB as strongest stimulator of MSC migration, we tested the injectable FB/HA formulation and HA-Tyr hydrogels with different cross-linking densities for their ability to allow cell migration and support chondrogenic differentiation *in vitro*. Finally, a bovine osteochondral explant model was used as hydrogel testing platform to monitor the recruitment of endogenous cells to the injury site in an *in vivo* mouse model.

## MATERIAL AND METHODS

### Cell isolation and culture

Bone marrow aspirates were collected from 6 patients undergoing total hip replacement (age 50-78 years) after informed consent (approved by the local Medical Ethical Committees of Erasmus MC: protocol MEC-2015-644; and Albert Schweizer Hospital: protocol 2011.07). Mesenchymal stem cells were isolated from leftover iliac crest bone chip material obtained from 1 patient (age 13 years) undergoing alveolar bone graft surgery (as leftover material with approval of local Medical Committee of Erasmus MC: MEC-2014-16). Human bone marrow stromal cells (hBMSCs) were expanded at a seeding density of 2,300 cells/cm<sup>2</sup> in alpha-Minimum Essential Medium ( $\alpha$ -MEM; Gibco, Carlsbad, California, United States) supplemented with 10% fetal bovine serum (FBS, Gibco, Carlsbad, California, United States), 50  $\mu$ g/mL gentamycin (Gibco, Carlsbad, California, United States), 1.5  $\mu$ g/mL fungizone (Gibco, Carlsbad, California, United States), 1 ng/mL fibroblast growth factor 2 (FGF2; AbD Serotec, Puchheim, Germany) and 25  $\mu$ g/mL ascorbic acid-2-phosphate (AA-2-P, Sigma-Aldrich, Saint Louis, MO). Medium was renewed twice a week. Passage 3 or 4 hBMSCs were used for *in vitro* experiments.

### Synthesis of Fibrinogen-HA and HA-Tyramine conjugates and hydrogel formation

FB/HA conjugates were synthesized by the reaction of a buffered fibrinogen solution with a HA-active ester solution using HA molecular weight of 235kDa (LifeCore Biomedical, LLC, Chaska, MN, USA) at FB/HA w/v ratio of 3.2:1 (6.25mg/mL and 1.96mg/mL respectively, ProCore Ltd. Ness Ziona, Israel) [60]. For hydrogel formation, a thrombin solution (50U/mL, Sigma-Aldrich, Missouri, USA) containing calcium chloride (1M CaCl<sub>2</sub>) was mixed to FB/HA conjugate and vortexed, that was polymerized at 37°C for 30 minutes. A similar formulation of FB/HA hydrogel, containing higher molecular weight HA, is approved for clinical use for the treatment of Osteoarthritis and associated pain ([www.RegenoGel.com](http://www.RegenoGel.com) by ProCore Ltd, Israel).

HA-Tyramine was synthesized as previously described [70]. Briefly, sodium hyaluronate (500mg, 1.25mmol of carboxyl groups, 280/290 kDa, Contipro Biotech S.R.O., Dolni Dobrouc, Czech Republic) was dissolved in deionized H<sub>2</sub>O (1% w/v) and were used for amidation reactions of carboxylic acid groups of HA with amine groups of Tyr. HA-Tyramine conjugates were prepared in a one-step reaction by adding 23.4 mmol 4-(4,6-dimethoxy-1,3,5-triazin-2-yl)-4-methylmorpholinium chloride (DMTMM, TCI Europe) as coupling agent and subsequently 25 mmol tyramine hydrochloride (Tyr, Sigma Aldrich, Buchs, Switzerland) dropwise to the solution. After precipitation, lyophilization and reconstitution in PBS, UV-vis analyses were performed to confirm

substitution of tyramine on HA ( $DS_{mol}$  14%). In a typical setup for hydrogel formation, freshly prepared solution of 0.5 U/ml HRP in phosphate buffered saline (PBS) was added to an aqueous solution of 3.5% (w/v) of HA-Tyr conjugates, and rotated overnight at 4 °C. To induce hydrogel formation, different  $H_2O_2$  concentrations (150, 300, 600  $\mu$ M) were added and immediately vortexed to form HA-Tyr hydrogels with different cross-linking densities (HA-Tyr 150, HA-Tyr 300 and HA-Tyr 600, respectively), in order to provide a homogeneous distribution within the pre-hydrogel solution before gelation occurs. The concentrations of  $H_2O_2$  were determined based on cross-linking density achievement and cell survival [59].

For the screening of factors to stimulate migration of MSCs, rat tail collagen I hydrogel (Life Technologies, Carlsbad, California, United States) was used. Briefly, 0.6% w/v Collagen hydrogels were prepared on ice by mixing 10X PBS,  $dH_2O$  and 1N sodium hydroxide (NaOH) and incubating at 37°C, 5%  $CO_2$ , for 30–40 minutes until a firm gel was formed, according to manufacturer's instructions.

### Rheological measurements

For rheological study, all hydrogels (400 $\mu$ L) were prepared in 12 well plates. Oscillatory tests (amplitude and time sweep) were performed at 37°C using an Anton-Paar MCR-302 rheometer equipped with a Peltier controller and 25mm plate-plate geometry. To monitor shear elastic moduli ( $G'$ ) and loss of moduli ( $G''$ ) of the hydrogels a humid chamber was created by placing water drops around the rheometer platform containing the gels removed from the plates and a chamber cover on top. The storage modulus ( $G'$ ) was measured at a strain of 1%, which was determined to be within the linear viscoelastic region.

### Swelling ratio studies and mesh size calculation

200 $\mu$ L hydrogel disks were swollen in PBS for 72h at 37°C. Then the hydrogel were gently blotted dry with Kimwipe and weighed immediately after. The disks were lyophilized overnight to obtain the dry weight. The swelling ratio was calculated by the following equation:

Swelling ratio ( $QM$ )=  $W_s/W_d$

where  $W_s$  is the swollen weight and  $W_d$  is the dry weight

The mesh size of HA-Tyr 150, 300 and 600 was calculated based on equilibrium swelling theory, using Flory-Rehner model, as reported by Leach [107-109]. The average molecular weight between crosslinks,  $M$ , was calculated using a simplification of the Flory-Rehner equation:

$$Q_v^{5/3} \cong \frac{vM_c}{V_1} \left( \frac{1}{2} - \chi \right)$$

where  $Q_v$  is the volumetric swelling ratio,  $v$  is the specific volume of the dry polymer,  $M_c$  is the average molecular weight between crosslinks,  $V_1$  is the molar volume of the solvent (18 mol/cm<sup>3</sup> for water), and  $\chi$  is the Flory polymer solvent interaction parameter.

$Q_v$  was determined from the degree of mass swelling ratio,  $Q_M$ :

$$Q_v = 1 + \frac{\rho_p}{\rho_s} (Q_m - 1)$$

where  $\rho_p$  is the density of the dry polymer (1.229 g/cm<sup>3</sup>) and  $\rho_s$  is the density of the solvent (1 g/cm<sup>3</sup> for water).  $Q_M$  values were determined experimentally and used to calculate  $Q_v$ .

The value of  $\chi$  for HA was estimated to be 0.473, based on several assumptions. First, it was assumed that  $\chi$  for HA is comparable to that for dextran, a well-studied polysaccharide, because HA and dextran have similar chemical structures. Furthermore,  $\chi$  estimates for HA that were based on an analysis similar to those published by Gekko [110] gave values within 2% of the value of  $\chi$  for dextran. Finally, differences between soluble, unmodified polysaccharides and crosslinked polymers were assumed to be negligible.

The swollen hydrogel mesh size,  $\xi$ , was determined with the following equation [109, 111]:

$$\xi = 0.1748 \sqrt{M_c} Q_v^{1/3}$$

Due to approximations made in the Flory-Rehner calculations, the values calculated (e.g.  $M_c$ ,  $\xi$ ) were considered approximations. However, these values were useful for making magnitude order comparisons of the HA-Tyr chemistries in biologically relevant features, such as mesh size.

### ***In vitro* 3D spheroid-based migration assay**

3D spheroid migration assay was used to evaluate cell migration as a function of different chemoattractants and varying concentrations of hydrogel. Micro-molds (Micro Tissues 3D Petri Dish, Sigma Aldrich, Missouri, USA) were used to cast 3D agarose Petri Dish, in order to form uniform size spheroids (Fig. 1A). Each micro-mold forms 256 circular micro-wells (diam. 400  $\mu$ m x 800  $\mu$ m) in a 16 x 16 array. After gelation, the agarose micro molds were placed in a 12 well-plate and equilibrated with  $\alpha$ -MEM supplemented with 10%FBS, 25ug/ml AA-2P at 37 °C, 5% CO<sub>2</sub> for 1h. In parallel, hBMSCs (1x10<sup>6</sup> cell/ml) were fluorescently labelled according to the manufacturer's instructions (Vybrant CFDA-SE Cell tracer Kit, Thermo Fisher, Carlsbad, California, United States). Suspensions of CFDA-SE labelled hBMSCs (1.28x10<sup>5</sup> cells) were seeded into each agarose micro-mold and incubated at 37 °C, 5% CO<sub>2</sub> for 24h in culture media, in order to form spheroids

containing 500 cells per micro-well. The next day, spheroids formation was assessed using a standard inverted microscope to exclude the 3D Petri dishes containing uneven size spheroids or the presence of individual cells. To collect spheroids, the micro molds were inverted in a new 12 well-plate containing  $\alpha$ -MEM supplemented with 1% insulin, transferrin and selenium (ITS+, Sigma Aldrich, Missouri, United States), 25 $\mu$ g/mL AA-2P (called from now on serum free medium, SF) and centrifuged for 5 minutes at 120g. The SF medium containing the harvested spheroids was transferred in falcon tube and centrifuged for 30sec at 300g to remove the supernatant. Then spheroids seeding was done after partial gelation on collagen gel (as it gels slowly), in order to avoid spheroids settling to the bottom of the gel and consequently fusion. Chambers slides (Nunc cell culture imaging 8 wells; Thermo Fisher, Carlsbad, California, United States) were used to polymerize collagen gel, 125 $\mu$ l were added to each well (9.4mm and 10.7mm in size with a thickness of 1.2mm).

In FB/HA and HA-Tyr hydrogels (HA-Tyr 150, 300 and 600), the spheroids were uniformly resuspended in the hydrogel prior to gelation. As these hydrogels polymerize rapidly, there was no problem of spheroid settling or fusion. 1mL containing 240 spheroids was transferred into each well of 12 well-plate (diameter of 22.8mm and height of 2.4mm) and incubated for gelation at 37°C respectively for 30 min.

Collagen 1 hydrogels containing about 30 spheroids were cultured for 48h in SF medium in the presence or absence of 50 or 100ng/mL of chemokine (C-C motif) ligand 5 (CCL5/RANTES), stromal derived factor 1 (SDF-1) or platelet derived growth factor BB (PDGF-BB, Peprotech, NJ, USA); whereas HA-based hydrogels were cultured with or without addition of 50ng/mL PDGF-BB for 24h, 48h and 72h [112]. For FB/HA hydrogels, Aprotinin (500kIU/ml, Sigma Aldrich, Missouri, USA) was supplemented into the media to prevent early degradation during culture. To monitor cell migration, a confocal microscope was used (Leica SP5, 10X magnification, FITC channel). Through the z-stack option of the confocal microscope all the spheroids were imaged from the top to the bottom in order to consider every single cell path, enabling individual cells tracking (3D reconstruction, Suppl. Fig.1A). Cell migration area from the core was quantified by averaging automated counts from 5 random spheroids running a macro developed in house using Fiji image processing software. The macro developed in house measures the cell migratory area in 2D, by running the Z Project function the software projects at maximum intensity all the stacks acquired covering the whole 3D area (Suppl. Fig 1B). From these pictures the macro excludes the core and sprouting cells (red) and count the area of cell migrating from the core (green), making concentric circles of 10 $\mu$ m radius (yellow). The algorithm generated concentric circles, each of increasing 10 $\mu$ m radius and tracked the cells present in each of these circles. Then the area of migrating cells and distance of cells in each of these circles with respect to the core was calculated and the area of all migratory cells was summed up to get the total migratory area.



## HA-based hydrogels invasion assay

To better mimic cell infiltration from the periphery into the gel, all HA-based hydrogels were formed in the presence or absence of 100 ng/mL PDGF-BB, this concentration was chosen to on our initial dose-response experiment and on a previous study [112]. 1mL of hydrogel was polymerized into each well of 12 well-plate (diameter of 22.8mm and height of 2.4mm), then the hydrogel was cut in an equal quarter of a circle. Each quarter of 250 $\mu$ L of HA-based hydrogel with a thickness of 2.4mm was used for the invasion assay. Then the gels (250 $\mu$ L) were maintained in suspension in 50 mL falcon tubes for 3h at 37°C in 500 $\mu$ L of SF medium containing CFDA-SE labelled hBMSCs ( $5 \times 10^5$  cells) under gentle shaking to avoid cell settlement and to allow cell adhesion to the gels (n=3/group). Afterwards 1.5mL of fresh SF medium was added in each gel per tube and gels were cultured for 7 days at 37°C (Suppl. Fig. 2A). Medium was changed every second day. For cell ingrowth detection, all gels were imaged at confocal microscope. For HA-Tyr gels multiple z-stacks of 5 $\mu$ m intervals were acquired (10X magnification), whereas for FB/HA hydrogels due to the opacity, tile scans were performed in the center after cutting the hydrogel in the middle; cell infiltration was visualized in the FITC channel.

## PDGF-BB release from hydrogels

The release of PDGF-BB from HA-based hydrogels *in vitro* was assessed as previously described [113]. The selected dose of PDGF-BB used in this assay was similar to *in vivo* experiment (see paragraph 2.10). Briefly, 300 $\mu$ L of hydrogels (diameter of 10.7mm and thickness of 3.4mm) loaded with 2ng/ $\mu$ L PDGF-BB, were formed in 48 well-plates at 37°C. Then 600 $\mu$ L of buffer (PBS, 0.5%BSA) was added to the plate and incubated at 37°C for 7 days. At pre-determined time points – 0, 2h, 8h, 24h, 72h, 120h, 168h – half of the medium (300 $\mu$ L) was collected and replaced by the same volume of fresh medium. Cumulative release of PDGF-BB was measured by quantifying the chemokine in the medium using an ELISA kit (human PDGF-BB, DuoSet ELISA, R&D System, Minnesota, USA).

## hBMSCs encapsulation and chondrogenic differentiation in HA-based hydrogels

Briefly, hBMSC-FB/HA and hBMSC-HA-Tyr suspensions were mixed with thrombin solution and with 0.5U/mL HRP and varying concentrations of H<sub>2</sub>O<sub>2</sub> (150, 300, 600  $\mu$ M) respectively, to form cell-hydrogels constructs with a cell density of  $3 \times 10^6$  cells/mL in 12 well-plates. After gelation for 30 min, the constructs were cultured in complete chondrogenic medium (CCM) for four weeks (day 0 was used as control); medium was changed every second day. The CCM consisted in Dulbecco's modified Eagle's medium with Glutamax (DMEM-HG; Gibco, Carlsbad, California, United States) supplemented

with 1% ITS, 50 µg/mL fungizone, 1.5µg/mL gentamicyn, 1mM sodium pyruvate (Gibco, Carlsbad, California, United States), 40µg/mL proline (Sigma Aldrich, Missouri, USA), 100nM Dexamethasone (Sigma Aldrich, Missouri, USA), 10ng/mL recombinant human transforming growth factor beta 1 (TGF-β1; R&D System, Minnesota, USA). The hBMSC used in this assay were isolated from patients undergoing total hip replacement and from the iliac crest chip of 1 patient. Samples were collected for RNA isolation or histological analysis on day 28.

### RNA isolation and qRT-PCR

After 28 days of culture, hBMSC/HA-Fibrin and hBMSC/HA-Tyr constructs were manually homogenized using a pellet pestle, further digested with hyaluronidase, and total RNA was extracted using the miRNeasy micro Kit (Qiagen, Hilden, Germany), according to the manufacturer's instructions. RNA concentration and quality were measured using NanoDrop ND100 UV-VIS spectrophotometer (Isogen Life Science B.V, de Meern, the Netherlands). cDNA was prepared using RevertAid First Strand cDNA Synthesis Kit (ThermoFisher, Carlsbad, California, United States) according to the manufacturer's instructions. qRT-PCR was performed in 20µL reactions on ABI Prism 7000 system (Applied Biosystem, Foster City, CA, USA) using either Taqman Universal PCR mastermix (Applied Biosystem, Foster City, CA, USA) or SyberGreen (Eurogentec, Seraing, Belgium). The expression of collagen type 2 (*COL2*) and aggrecan (*ACAN*) was determined. Glyceraldehyde-3-phosphate dehydrogenase (*GAPDH*) was selected as reference gene after comparison with other housekeeping genes [114]. Data were calculated as relative mRNA values.

### *In-vivo* subcutaneous osteochondral defect model

To evaluate the effect of the hydrogels on cartilage repair via ingrowth of endogenous cells, an *in vivo* subcutaneous mouse model was used. All animal experiments were approved by the local animal committee (EMC3284, protocol number 116-14-02). Osteochondral defects were created in osteochondral biopsies (8mm diameter, 5mm height) harvested from metacarpal-phalangeal joints of 3 to 8 months old calves as described previously [115]. Four mm diameter dermal biopsy punches (Stiefel Laboratories, Munich, Germany) and scalpels were used to create osteochondral defects. The defects in the osteochondral plugs were either left unfilled (empty) or filled with 50 µl FB/HA or HA-Tyr 150 hydrogels with or without 1µg/mL of PDGF-BB (n=5/group). In comparison to *in vitro* migration and invasion assay, a higher concentration of PDGF-BB was employed since the growth factor *in vivo* is expected to be released over several days and more easily degraded by proteases [68]. Osteochondral explants were covered with Neuro-Patch membrane (Braun, Melsungen, Germany) to prevent host cell ingrowth and were implanted subcutaneously in female NMRI nu/nu mice (Charles

River, Wilmington, MA, USA) under isoflurane anaesthesia. Four incisions were made on the dorsum of each animal, and subcutaneous' pockets were created using a blunt blade; one construct was placed in every pocket and the incisions were closed with wound clips.

After 4 weeks, mice were euthanized by cervical dislocation, the constructs carefully removed and fixed in 4% formalin for 5 days. Then samples were decalcified in 10% EDTA for two weeks, subsequently embedded in paraffin and subjected to histology (Thionin staining) or immunohistochemistry (Collagen type 2 deposition).

## Histology and Immunohistochemistry

Retrieved samples were embedded in paraffin and sectioned (6  $\mu\text{m}$  sections). Slides were deparaffinised and stained with Thionin to visualize glycosaminoglycans in the extracellular matrix. Briefly, slides were first stained with Thionin solution (0.04% Thionin in 0.01M aqueous sodium acetate, Sigma-Aldrich, Missouri, United States) for 8 min and differentiated in 70% ethanol for 8 sec. The cross-sectional area of the osteochondral defect, the number of the infiltrated cells and the area of newly formed Thionin positive tissue were determined using Fiji software (National Institutes of Health, Bethesda, MA, USA). Cell ingrowth into the hydrogels was assessed by counting the number of cell nuclei infiltrating the defect area of the cartilage layer (CL) and the defect area of the subchondral bone (SB) in Thionin stained cross-sections (n=5/group, n=3sections/sample). To convert RGB images in 8 bit we used a trainable weka segmentation plugin, in order to train the software to define the classes of area to exclude (different shadows of background, Thionin staining) and select the area of interest (in this case the cells nuclei). After extracting the results, we select the best threshold to extract the desired objects (cell nuclei). Cartilage formation was quantified as percentage of positive area by dividing the Thionin signal intensity in the defect (glycosaminoglycan deposition) by the defect area of the cartilage layer (CL) and the defect area of the subchondral bone (SB) as measured in full Thionin-stained cross-sections (n=5/group, n=3sections/sample). Fiji image processing software was used to identify areas using a protocol previously described [116].

For immunohistochemical analysis, deparaffinized sections from hydrogel samples were probed with mouse anti-human collagen type 2 antibody (II-II6B3, Developmental Studies Hybridoma Bank, Iowa City, IA, USA). Antigen retrieval was performed by incubation in 0.1% pronase (Sigma-Aldrich, Missouri, USA) in PBS for 30 min at 37°C. Then slides were incubated with 1% hyaluronidase (Sigma-Aldrich) in PBS for 30 min at 37°C and subsequently with 10% goat serum (Sigma-Aldrich) to block non-specific binding. The primary antibody against collagen type II (1:100 dilution) or mouse IgG1 negative control (Serotech Ltd, Oxford, UK) in PBS containing 0.1% BSA was incubated overnight at 4°C coupled with biotinylated F(ab)2-labeled goat-anti mouse secondary

antibody (#115-066-062; Jackson ImmunoResearch Europe) to prevent cross-reaction with mouse antigens. Excessive primary antibody was captured by addition of 0.1% normal mouse serum prior to the overnight incubation at 4°C with the sections. The reaction was catalyzed by an alkaline-phosphatase-label conjugate (Label, HK-321-UK, Biogenex, CA, USA) diluted 1:100 in PBS/BSA and visualized by subsequent incubation of Neu Fuchsin substrate (Chroma, Kongen, Germany). Slides were counterstained with Haematoxylin.

## STATISTICAL ANALYSIS

The results were expressed as mean  $\pm$  standard deviation (SD). For the 3D spheroids-based migration assay in collagen gel, experiments were performed using 4 different hBMSC donors and triplicate per donor, a linear mixed model was used for migratory cell area data. Multiple comparisons were analysed with Sidak post hoc test. Conditions and donors were considered as fixed and random parameters, respectively. Normal distribution of the data or the residuals of the data were confirmed by both Kolmogorov-Smirnov and Shapiro-Wilk tests. In the 3D migration assay in HA-hydrogels, experiments were performed using 3 different donors and triplicate per donor, data were not normally distributed and Kruskal-Wallis test was performed. For the quantification of cartilage repair in the osteochondral samples, experiments were performed using 5 explants per group and 3 sections per sample, statistically significant differences between untreated and hydrogel treated groups were determined by one-way ANOVA, Tukey test for multiple comparison. All tests were performed using SPSS software. Differences were considered statistically significant for  $p < 0.05$ .

## RESULTS

### Effect of different chemotactic factors on hBMSC spheroid migration in hydrogel

Although monolayer cell migration has commonly been used for migration studies, recent research shifted toward 3D culture as a more relevant biochemical and biomechanical microenvironment [117]. Here, we used a spheroid-based migration assay to examine the effect of chemotactic factors on the migration of hBMSCs. CDFA-SE fluorescently labelled hBMSC spheroids with an average diameter of 125  $\mu\text{m}$  were generated (Fig. 1 A), placed in a collagen hydrogel and cultured in the absence or in the presence of 50 or 100ng/ml PDGF-BB, RANTES or SDF-1. After 48h, cell migration was imaged (Fig. 1B). Exposure of SDF-1 (50 and 100ng/mL), PDGF-BB (50ng/mL) or RANTES (50ng/mL)

increased hBMSC migration compared to control ( $***p<0.001$ ,  $**p<0.01$ ,  $*p<0.05$ ), except for 100ng/mL RANTES, although variability among donors was observed (Fig. 1C). These results demonstrate that 50ng/mL of PDGF-BB was the most favourable of the tested factors based on higher tendency to increase among all tested donors.

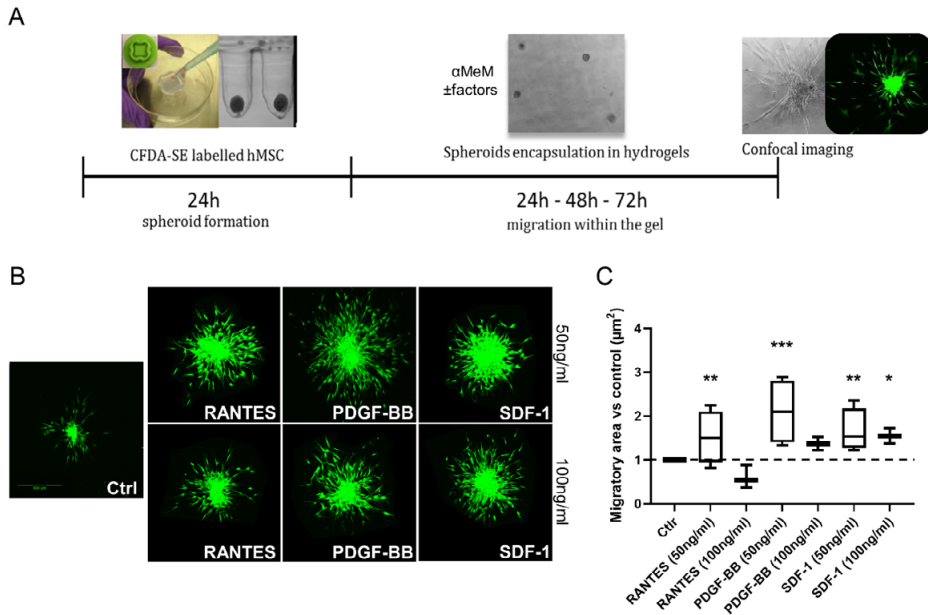


**Figure 1. Dose response-study of factors on hBMSCs migration in collagen hydrogel. A)** Scheme of 3D spheroids formation and migration assay in hydrogels. **B)** Representative images of BMSCs migrating from the spheroids core at 48h of culture in absence or in presence of 50 or 100ng/mL of RANTES, PDGF-BB or SDF-1; 10X magnification, scale bar indicates 500µm. **C)** Migratory area ( $\mu\text{m}^2$ ) of hBMSCs encapsulated in collagen hydrogel in absence or in presence of 50 or 100ng/mL of RANTES, PDGF-BB and SDF-1. Results from 4 hBMSC donors assessed in triplicate (donor 2) and quadruplicate (donors 1, 3 and 4) are shown;  $*p<0.05$ ,  $**p<0.01$ ,  $***p<0.001$

### PDGF-BB promotes hBMSC migration in FB/HA and HA-Tyr hydrogels with different cross-linking densities *in vitro*

In terms of physical impediment to 3D cell recruitment, the migration of CDFA-SE labelled hBMSCs was assessed in HA-Tyr hydrogels with different crosslinking densities (HA-Tyr 150, 300 and 600  $\mu\text{M}$   $\text{H}_2\text{O}_2$ ) and FB/HA hydrogel, with or without PDGF-BB exposure, using a 3D spheroid assay. Confocal imaging revealed that the area of cell migration from the spheroids in all HA hydrogels progressively increased over three days culture in the presence of 50ng/mL PDGF-BB, except for the stiffer HA-Tyr hydrogels (HA-Tyr 600, Fig. 2A, B) that showed no migration at all. FB/HA hydrogels supported the widest cell migration area in presence of PDGF-BB (4-fold increase compared to FB/HA

only hydrogels after 72h; Fig. 2A, B). In FB/HA gels the cells exhibited spindle-shaped morphology (Fig. 2B), which might have facilitated faster migration, whereas in HA-Tyr hydrogels (HA-Tyr 150, 300) cells showed populations of both spindle and rounded shaped morphology that might have reduced the migration ability.

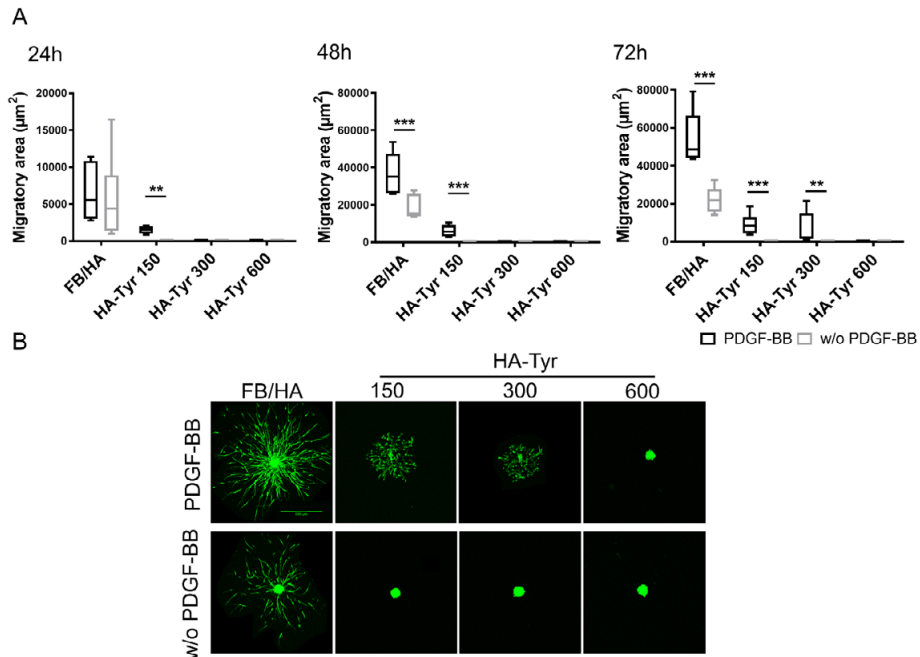


**Figure 2.** PDGF-BB induces progressive increase of cell migration in FB-HA and HA-Tyr with different crosslinking densities. **A**) Migratory area ( $\text{mm}^2$ ) of hBMSCs encapsulated in FB/HA and HA-Tyr 150, 300 and 600 at 24h, 48h and 72h of culture in absence or in presence of 50ng/mL of PDGF-BB. Results from 3 hBMSC donors assessed in quintuplicate are shown (\*\* $p < 0.01$  \*\*\* $p < 0.001$ ). **B**) Representative images of BMSCs migrating from the spheroids core at 72h of culture in absence or in presence of 50 and 100ng/mL of PDGF-BB; 10X magnification, scale bar indicates 500 $\mu\text{m}$ .

The migration in HA-Tyr hydrogels with different cross-linking density was found to be inversely correlated with the storage modulus of the hydrogel ( $G'$ ; Suppl. Fig. 2).

Increased migration in the presence of PDGF-BB was observed at 24h and 48h for HA-Tyr hydrogels with lower crosslinking (HA-Tyr 150), which were softer and fostered faster migration than stiffer gels (HA-Tyr 300, 600; \*\* $p < 0.01$  and \*\*\* $p < 0.001$  respectively; Fig. 2A). Based on the mesh size calculation described by *Leach et al.* [109], and assuming that HA-Tyr had the same density as HA, the mesh sizes were calculated to be  $184.99 \pm 8.03$ ,  $160.60 \pm 5.04$  and  $130.85 \pm 7.04$  nm for the HA-Tyr 150, 300 and 600, respectively. At increased cross-linking density, the mesh size decreased according to a decreased swelling ratio (Suppl. fig.3A. B), resulting in a reduced migration kinetic.

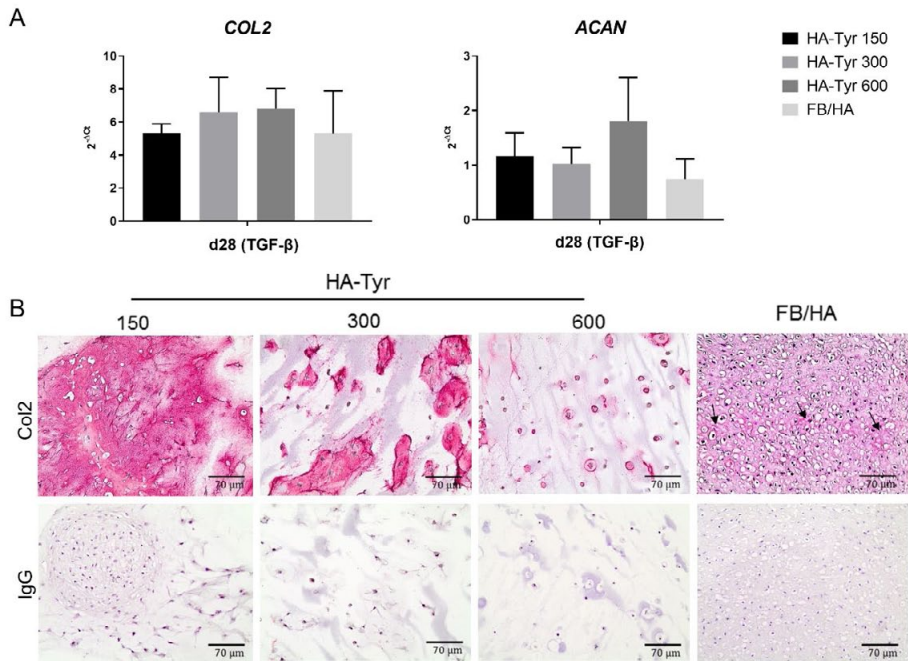


**Figure 3. The HA-hydrogels support chondrogenesis *in vitro*.** **A)** hBMSCs encapsulated in HA-Tyr 150, 300, 600 and FB/HA hydrogels were cultured for 28 days in chondrogenic medium in presence of TGF- $\beta$ 1. Relative mRNA levels of *COL2* and *ACAN* were assessed by qRT-PCR and normalized to GAPDH ( $2^{-\Delta Ct}$ ). Data are from 1 hBMSCs donor and presented in biological triplicate as means $\pm$ SD. **B)** Immunohistochemical staining of collagen type II assessed in all hydrogel groups after 28 days of culture in chondrogenic medium in presence of TGF- $\beta$ 1. In FB/HA and HA-Tyr hydrogels the collagen type II deposition is presented by the pink staining (black arrows in FB/HA hydrogel). IgG isotype controls demonstrate collagen type II specificity. 10X magnification, scale bar indicates 70 $\mu$ m.

To better mimic the process of hydrogel invasion by endogenous cells, CDFA-SE labelled hBMSCs in suspension were incubated with free-floating HA-based hydrogels, polymerized with or without 100ng/mL of PDGF-BB, then cultured for 7 days (Suppl. Fig. 4A). Imaging of the hydrogels at day 7 suggested higher cell infiltration in FB/HA hydrogel with PDGF-BB compared to FB/HA only. In HA-Tyr hydrogels, cell migration looks to be higher in presence of the chemokine rather than without and dependent of crosslinking densities (Suppl. Fig. 4B).

### HA-based hydrogels support chondrogenesis *in vitro*

With the aim to investigate whether FB/HA and HA-Tyr-hydrogels are suitable for cartilage engineering purposes, their ability to support chondrogenic capacity of hBMSCs was evaluated. hBMSC-loaded hydrogels were cultured for 28 days in CCM and gene expression at day 0 was used as control; hBMSC differentiation was further assessed by IHC. At day

0 gene *COL2A1* expression was undetectable and *ACAN* expression was very low with Ct values between 34 and 37. The results indicate that hBMSC-FB/HA and hBMSC/HA-Tyr constructs similarly allowed chondrogenic differentiation, as demonstrated by clear cartilage marker expression at day 28 (Fig. 3A). Immunohistochemical staining for type II collagen confirmed that FB/HA constructs exhibited areas of newly synthesized matrix and cells with a chondrocyte-like morphology (i.e. rounded and residing within lacunae Fig. 3B). Interestingly, type II collagen deposition in HA-Tyr hydrogels was limited to the pericellular space except for HA-Tyr 150 where the staining was diffuse in the matrix (Fig. 3B), indicating an inverse relationship between the cross-linking density and the extent of neo-cartilage tissue deposition. Since improved cell migration and cartilage matrix formation were observed in HA-Tyr hydrogels with the lowest cross-linking density, HA-Tyr 150 and FB/HA hydrogels were selected for further *in vivo* experiments.

### **FB/HA hydrogels improve endogenous cartilage tissue repair in an *in vivo* subcutaneous model**

To evaluate the ability of the selected hydrogels to support endogenous cartilage repair *in vivo*, osteochondral explants with simulated defects were filled with FB/HA and HA-Tyr, both loaded or not with PDGF-BB, and implanted subcutaneously in nude mice (Fig. 4A). After 4 weeks, osteochondral explants were collected and analyzed by histology. Data revealed differences between the groups in number of cells colonizing the defect through full-depth cartilage and subchondral bone (Fig. 4B, C, Suppl Fig. 5). While cells were evenly distributed throughout the whole area of FB/HA gels (both cartilage and subchondral zone), cell ingrowth was limited to the periphery in HA-Tyr gels in the vast majority of the gels (Fig 4B). Cell infiltration was significantly higher in the cartilage layer and subchondral bone of FB/HA gel group without PDGF-BB compared to HA-Tyr group without PDGF-BB (\* $p < 0.05$  and \*\*\* $p < 0.001$ : Fig. 4C). Scarce cell infiltration was noticed in only 2 out of 5 samples in the empty defect group (data not shown). When FB/HA and HA/Tyr hydrogels were loaded with PDGF-BB, no significant differences in endogenous cell ingrowth were observed in comparison to untreated hydrogels (Fig. 4C), despite approximately 35% of PDGF-BB was released in FB/HA after one week *in vitro* (Suppl. Fig. 6). This suggest that the factor release did not exert any appreciable effect on migration in the hydrogels (Fig. 4B, C).

In addition to higher cell infiltration in FB/HA gels, cell mediated matrix production was significantly enhanced in the cartilage areas of untreated FB/HA gels in comparison to HA-Tyr gels (\* $p < 0.05$ , Fig 4B, D). The subchondral bone areas showed similar GAG production and no statistical differences were observed. Interestingly, the addition of PDGF-BB to FB/HA gels inhibited cartilage formation (\* $p < 0.05$ , Fig. 4B, D), while in HA-Tyr gels no significant differences were observed when PDGF-BB was added (Fig.



4B, D). Finally, deposition of type II collagen *in vivo* confirmed a similar pattern to GAG deposition (Fig. 4E).

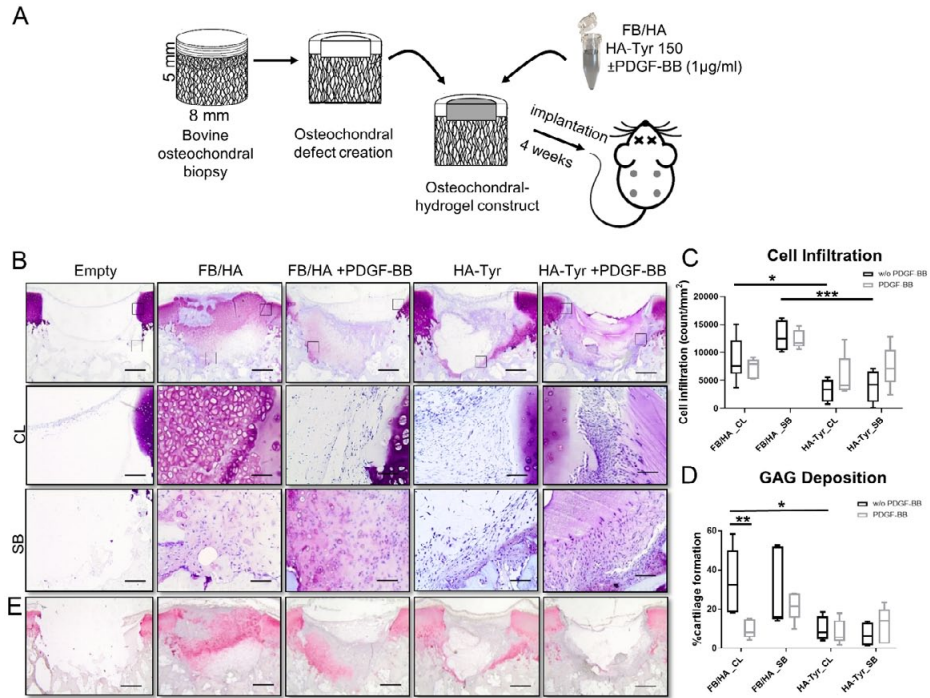


**Figure 4. Improved tissue repair of osteochondral defects filled with HA-based hydrogels in an *in vivo* subcutaneous tissue model.** **A)** Scheme of an osteochondral repair explant filled with FB/HA and HA-Tyr 150 hydrogel in presence or absence of 1µg/mL of PDGF-BB, implanted in the subcutaneously in athymic mice. **B)** Representative images of the repair constructs stained with Thionin (pink=GAG) showing cells and matrix deposition within the osteochondral defects after 4 weeks of implantation. 10X magnification scale bars indicate 1mm and 70µm, respectively. **C)** Cell infiltration (count per mm<sup>2</sup>) in the CL and SB layers of the osteochondral defects \*p<0.05, \*\*p<0.01 and \*\*\*p<0.001. **D)** Percentage of cartilage formation in hydrogels indicated by GAG deposition in CL and SB. \*p<0.05 and \*\*p<0.01. **E)** Representative images of repair constructs stained with Collagen type II by immunohistochemistry after 4 weeks of implantation. 10X magnification; scale bars indicate 1mm.

## DISCUSSION

In this study we compared different types of HA-containing hydrogels for their capacity to support cell migration and chondrogenesis of hBMSC *in vitro*, and to promote recruitment of endogenous cells to the wound site, followed by cartilage repair in an osteochondral defect model *in vivo*. We showed that the FB/HA conjugated formulation

enhanced a spontaneous cellular healing response and was more supportive for cartilage repair compared to the HA-Tyr hydrogel. In addition, the provision of PDGF-BB, chosen as the most favorable chemotactic agent, did not increase cell infiltration into the tested hydrogels but impaired chondrogenesis *in vivo*.

Our approach is based on the use of an advanced platform employed as a pre-clinical tool to screen new biomaterials and biomolecules for their potential to support endogenous cartilage repair. The advantage of this strategy is the application of more relevant experimental models due to the use of an *in vitro* 3D spheroids-based migration assay and an osteochondral defect model, which bring our approach a step closer to physiologically relevant systems. This could be widely applied to achieve stronger experimental evidence of the not well-characterized dynamic process of cell homing and to uncover the delicate step of early cell migration into biomaterials.

The ideal hydrogel should allow cell adhesion, migration and differentiation to favor the synthesis of extracellular matrix components necessary to mimic the native properties of cartilage. However, tuning the gels to match not only cartilage composition and architecture but also mechanical properties to sustain the load, may prevent cell ingrowth that is necessary for the first steps of endogenous tissue repair. Consistent with other *in vitro* studies [59], we found that changes in mechanical properties influenced cell spreading, migration and differentiation. The modulation of HA-Tyr cross-linking degrees (150, 300 and 600  $\mu\text{M}$   $\text{H}_2\text{O}_2$ ), while keeping HA-Tyr and HRP concentrations constant, was the major determinant for both cell migration and matrix synthesis during hBMSC chondrogenesis.

The resulting hydrogels ranged in storage modulus from 80 to 3,000 Pa, which mimics the mechanical properties of certain native cartilaginous tissues like the nucleus pulposus of the intervertebral disc (3-8kPa; [118]), but is lower than the value reported for bovine adult cartilage (range 300-800kPa, [119]). However, cell migration was inhibited in HA-Tyr 600 hydrogels, indicating cell spreading limitations in stiffer highly crosslinked materials [120]. These stiffer gels, however, also have lower mesh size. In general, migration was strongly dependent on crosslinking, indeed gels with low crosslink density have both lower stiffness and higher mesh size (HA-Tyr 150), and foster faster migration; albeit the migration was always less in HA-Tyr than in FB/HA gels. Despite the similar stiffness ( $G'$ ) of FB/HA and HA-Tyr 150, cell migration was profoundly affected by the different HA concentration as well as by the different network and the presence of components that improve cell adherence.

To ameliorate cell migration on HA-Tyr hydrogels further cues could be implemented, such as the Arg-Gly-Asp (RGD) binding sequences to improve the integrin-mediated cell attachment [121].

Chondrogenesis occurred in all tested hydrogels, as indicated by comparable gene expression levels of *COL2* and *ACAN*. While FB/HA, HA-Tyr 150 and 300 hydrogels

showed collagen type II-rich matrix production, HA-Tyr 600 microenvironments showed only pericellular collagen type II deposition. Previous works [59] demonstrated extensive collagen type II deposition in the newly formed HA-Tyr matrix. Although  $G'$  values of our gels were much lower (0.08 and 0.45kPa in HA-Tyr 150 and 300, respectively), this suggests that mechanical stiffness is not the only factor that influences stem cell fate [122]. It is possible that the higher amount of HA-Tyr used to form the hydrogel (3.5%w/v vs 2%w/v) increased its density, which has been shown to negatively affect matrix deposition by hBMSCs [123]. Furthermore, the higher concentration may have increased its viscosity, which in turn may have hindered the diffusion of nutrients and growth factors in all the HA-Tyr constructs, which is known to influence the effectiveness of hBMSC chondrogenesis [124], thereby decreasing GAG deposition. The combination of those factors may have decreased the ability of those hydrogels to allow migration and support matrix accumulation. To further support our observations, a recent study has shown that increased HA crosslinking density resulted in an overall more restricted matrix distribution while detecting no statistically significant differences in collagen type II expression among all the groups [125].

Consistently with other reports [68, 126], we found that PDGF-BB was the most effective chemoattractant of hBMSCs in hydrogels, among the factors tested. PDGF-BB is a well-known mitogen and we cannot thus completely rule out a contribution of cell proliferation in the 3D spheroid *in vitro* assay. Nevertheless, cells that detached from the core were identified as migrating cells and proliferation did not influence this measurement as it would have been reflected as an increased the size of the core. It should also be considered that both processes are desirable and necessary in a context of endogenous tissue repair *in vivo* to guarantee proper cell colonization of the site of injury.

It is worth noting that the PDGF-BB gradient enhanced short-term spheroid migration *in vitro* (3 days) and improved cell infiltration of hydrogels at 7 days of culture in HA-based hydrogels. Our release study of PDGF-BB over 7 days suggested that a chemotaxis gradient might have been less pronounced within HA-Tyr hydrogels than with FB/HA gels. Earlier studies exploring the influence of mechanical strength of HA-Tyr hydrogels on protein release demonstrated that release profile of the molecules depended on mesh size, with the release rate decreasing with decrease in mesh size [105]. The higher concentration of HA within HA-Tyr hydrogels, however, might also have increased the electrostatic interactions among their hydrophilic groups and the charged amino acid residues of the PDGF-BB [127], impeding a sustained delivery.

Although 3D migration studies can provide valuable information, the majority of conventional *in vitro* hydrogel culture systems do not recapitulate the native tissue properties [128]. Furthermore, a recent study has shown that BMSC gives a distinct response when placed in a different environment, demonstrating that the

microenvironment plays an important role in the induction of cell differentiation highlighting its importance when evaluating the applicability of biomaterials for cartilage repair [129]. Therefore, a fundamental prerequisite is the testing of 3D cell migration and differentiation in a more relevant osteochondral-like system, in order to closely mimic a joint-like microenvironment. To validate our *in vitro* findings, FB/HA and HA-Tyr 150, with or without PDGF-BB, were placed in osteochondral defects in an explant model and implanted subcutaneously *in vivo*. Cellular invasion was evident by 4 weeks in both hydrogels, though infiltration was most advanced in the FB/HA hydrogels, which allowed a uniform distribution of cells. Interestingly, the bridging tissue in the untreated FB/HA constructs, closing over 85-90% of the osteochondral gap compared to HA-Tyr hydrogels, resulted also in increased cartilage matrix formation (\* $p < 0.05$  and \*\* $p < 0.01$ ), and subsequently more collagen II. A possible explanation for the extensive differences in cell infiltration between the FB/HA and HA-Tyr hydrogels might be that the high fibrin content (FB/HA 3.2:1) favoured binding of cells to its 3D architecture and accelerated cell migration in the porous clots containing hyaluronan [130]. The HA in the FB/HA hydrogels may have influenced the behavior and function of cells involved in the remodeling of the damaged tissue [131]. Whereas the high content of low molecular weight HA (280kDa) in the HA-Tyr gels may have acted as a barrier to cell adhesion and migration [132], therefore slowing this process. We also noticed that 2 out of 5 osteochondral empty defects implanted as controls were partially colonized by cells. Despite the presence of a membrane patch it is possible that liquid or blood after surgery reached the osteochondral defects. Indeed, part of the infiltrated cells were red blood cells. Furthermore, as the bovine explants were harvested from calves aged 6-8 months, the young and healthy material is likely to provide a favorable environment for repair.

This study showed a reduction in the size of cartilage lesion and enhanced regeneration of the cartilage using FB/HA hydrogels without exposure to growth factor before implantation. Interestingly, addition of PDGF-BB worsened the repair of cartilage. A previous study on osteochondral repair in a rat model, demonstrated no significant presence of cartilage matrix deposition when the defect was filled only with PDGF-BB loaded in heparin-conjugated fibrin gels [68]. Although this study used higher concentrations of PDGF-BB (8.5 $\mu\text{g}/\text{mL}$  and 17 $\mu\text{g}/\text{mL}$ ) compared to the present study (1 $\mu\text{g}/\text{mL}$ ), these findings are in line with our observations, suggesting that the presence of PDGF-BB, although not influencing cell recruitment, diminished chondrogenic differentiation leading to more fibrous tissue formation. Future studies will be performed to evaluate a dose-dependent effect of PDGF-BB on cartilage repair after *in vivo* transplantation and explore the efficacy of other chemotactic agents [66]. To further improve the quantity or quality of the matrix produced by the recruited cells,

our system can be functionalized, for example by adding pro-chondrogenic factors [133, 134], that can stimulate cartilage formation or inhibit hypertrophy.

Our findings with the osteochondral explant model are partially in line with clinical outcomes of the microfracture procedure [16, 135]: cells are recruited without supplementation of exogenous factors and spontaneously generate a cartilaginous tissue, albeit this is a mixed hyaline/fibrous tissue with non-favorable long term outcome. Although the origin of these reparative cells needs further analysis, we suppose that the migrating cells are either endogenous stem/progenitor cells from the subchondral bone region, either perivascular or bone lining cells, that have differentiated towards the chondrocyte lineage, since the newly generated tissue was GAG and collagen type II positive. It is clear that the construct is revascularized upon implantation, meaning a connection is made with the mouse system [136]. Hence, we cannot exclude the presence of cells from murine origin in our plugs. Further investigations of the origin of these cells would be interesting, although this poses significant challenges in discriminating mouse and bovine cells in decalcified sections.

Subcutaneous implantation does not entirely recapitulate the diarthroidal joint in terms of cellular components, immunologic response and mechanical stimuli and allows only short-term evaluation of cell colonization and matrix production *in vivo*. To study the effect of mechanical stimuli to our endogenous cartilage repair system, the use of a bioreactor system to simulate physiological joint kinematics *in vitro* can be useful [137]. Multiaxial loading was shown to induce production and activation of transforming growth factor-beta (TGF- $\beta$ 1), thereby promoting chondrogenesis of BMSCs [138]. Since the process of endogenous cartilage repair and the involved cell populations are still not well characterized, this system can be implemented to carry out additional studies including pre-clinical screening of targeted therapies and biomaterial-based implants. Eventually, the long-term therapeutic effects will need to be validated in large animal models of osteochondral injury.

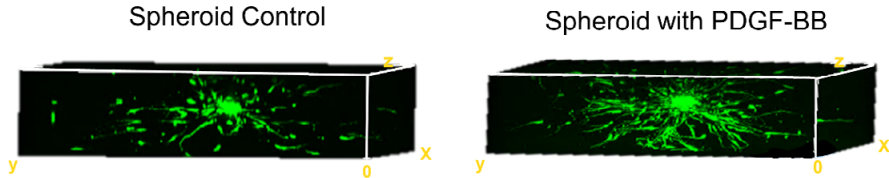
## CONCLUSION

The manuscript emphasizes the application of an advanced preclinical biomaterial testing platform to select the most promising hydrogel to support cell migration and differentiation for cartilage regenerative strategies, posing interesting features in the use of FB/HA conjugated hydrogel, even in the absence of the factor stimulating migration. It is worth noting that both *in vitro* and *vivo* findings indicate that in the FB/HA hydrogel the use of stimulating factors was not necessary to create a local ECM microenvironment amenable for endogenous cell recruitment in both cartilage and bone layers. Particular consideration should be given on creating an environment where

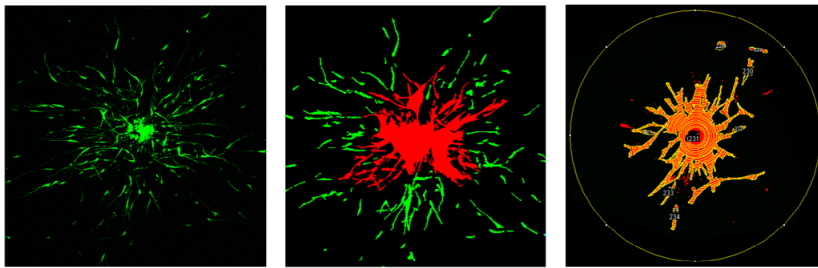
cues may be introduced to stimulate matrix deposition and improve the quality of the newly-formed cartilage, e.g. by silencing anti-chondrogenic factors [139], and promote proper collagen fiber alignment [140]. Combination of these processes will lead to an ideal situation where different but complementary regulators create an optimal microenvironment for cartilage repair.

## SUPPLEMENTARY DATA

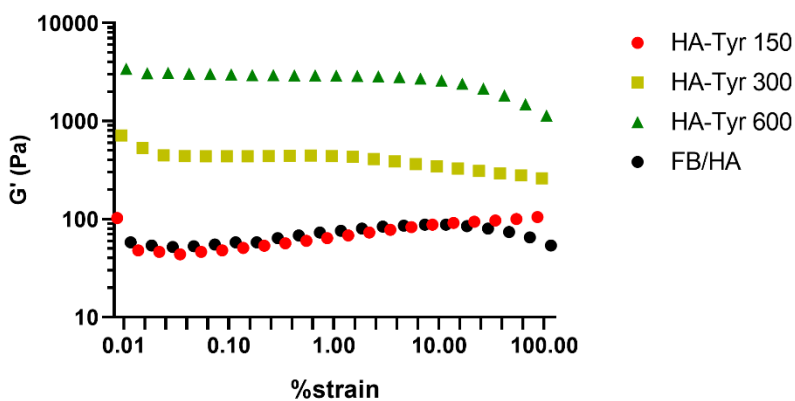
A



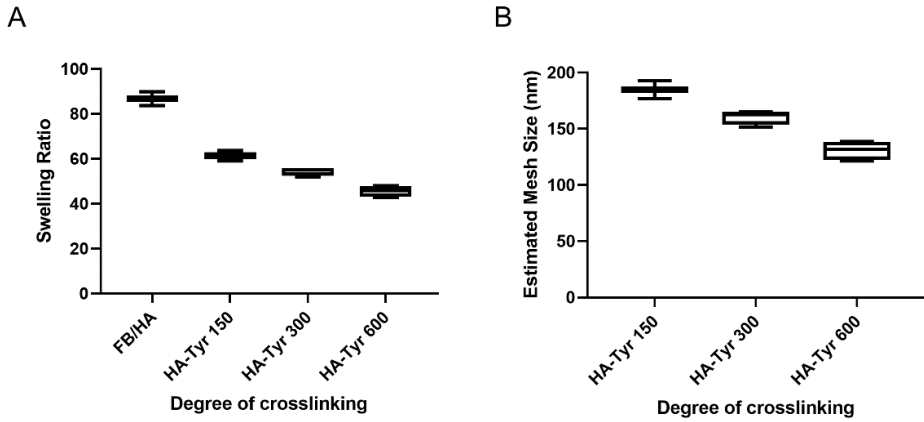
B



**Supplementary Figure 1. Decomposition of a single spheroid after 72h of migration. (A)** Representative images of spheroids cultured with and without PDGF-BB, 3D reconstruction using Fiji software. **(B)** Representative image of spheroid to distinguish core and sprouting cell (red) and migrating cells (green). Concentric circles of 10 $\mu$ m radius to calculate the migrating cells and distance of cells with respect to the core to obtain the total migratory area (yellow).

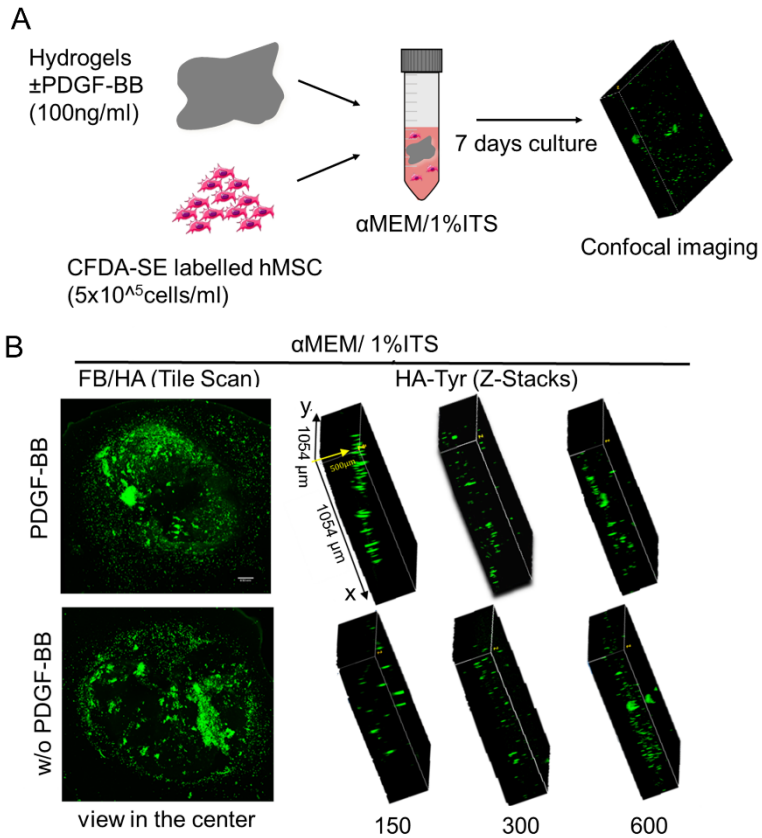


**Supplementary Figure 2. Rheological measurement.** Typical evolution of the storage modulus  $G'$  of HA-Tyr hydrogels formed with 0.5U/ml of HRP and cross-linked at varying concentrations of  $H_2O_2$ , and FB/HA hydrogels. The measurement was taken with constant deformation of 1% at 1Hz and 37°C.

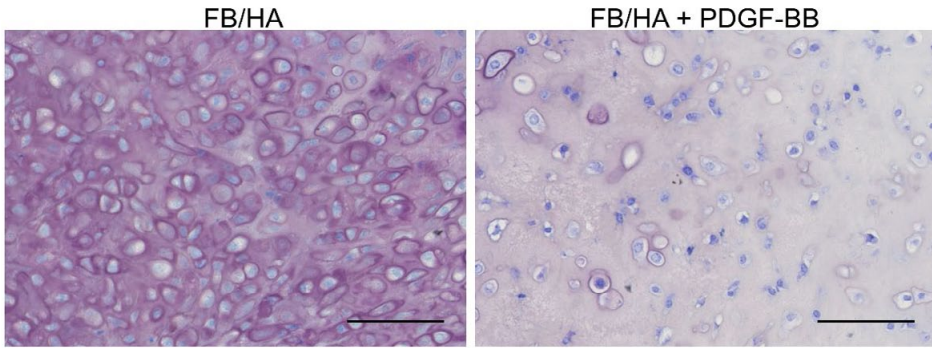


**Supplementary Figure 3. Effect of crosslinking degree on swelling ratio and mesh size. (A)** Crosslinking degree of FB/HA and HA-Tyr hydrogels at varying concentrations of  $H_2O_2$  modulate the equilibrium swelling ratio. Hydrogels were swollen for 72h at 37°C. Means $\pm$ -SD; n=4/group. **(B)** Estimated mesh size calculation based on equilibrium swelling theory. Means $\pm$ -SD; n=4/group.





**Supplementary Figure 4. HA-hydrogels allow hBMSCs ingrowth *in vitro*.** (A) Scheme of cell invasion assay, hBMSC together with hydrogels (polymerized in presence or absence of PDGF-BB) maintained in culture. (B) Representative images of cells invasion into HA-Tyr hydrogels formed with 0.5U/ml of HRP and cross-linked at varying concentrations of H<sub>2</sub>O<sub>2</sub>, and FB/HA hydrogels after 7 days of culture. Scale bars indicate x=1054  $\mu$ m, y=1054  $\mu$ m, z=500 $\mu$ m



**Supplementary Figure 5. FB/HA hydrogels remodeling in osteochondral defect explants after *in vivo* subcutaneous implantation.** Representative images of FB/HA in absence or presence of PDGF-BB stained with Thionin (pink=GAG). Cells, nuclei and matrix deposition are distinguishable within the osteochondral defect after 4 weeks implantation. 20X magnification; scale bars indicate 100  $\mu$ m.